Partial topological Zak phase and dynamical confinement in a non-Hermitian bipartite system

X. Z. Zhang[1] and Z. Song[2,*]
[1]*College of Physics and Materials Science, Tianjin Normal University, Tianjin 300387, China*
[2]*School of Physics, Nankai University, Tianjin 300071, China*

(Received 20 August 2018; published 15 January 2019)

Unlike a Chern number in a two-dimensional (2D) and 3D topological system, the Zak phase takes a subtle role to characterize the topological phase in 1D. On the one hand, it is not gauge invariant, and, on the other hand, the Zak phase difference between two quantum phases can be used to identify the topological phase transitions. A non-Hermitian system may inherit some characters of a Hermitian system, such as entirely real spectrum, unitary evolution, topological energy band, etc. In this paper, we study the influence of a non-Hermitian term on the Zak phase. We show exactly that the real part of the Zak phase remains unchanged in a class of 1D bipartite lattice systems even in the presence of the on-site imaginary potential. The non-Hermitian term only gives rise to the imaginary part of Zak phase. Such a complex quantity has a physical implication when we consider the dynamical realization in which the Zak phase can be obtained through adiabatic evolution. In this context, its imaginary part represents the amplification and/or attenuation of the Dirac norm of the evolved state. Based on this finding, we investigate a scattering problem for a time-dependent scattering center, which is a magnetic-flux-driven non-Hermitian Su-Schrieffer-Heeger ring. Due to the topological nature of the Zak phase, the intriguing features of this design are the wave-vector independence and allow two distinct behaviors, perfect transmission or confinement, depending on the timing of a flux impulse threading the ring. When the flux is added during a wave packet travelling within the ring, the wave packet is confined in the scatter partially. Otherwise, it exhibits perfect transmission through the scatter. Our finding extends the understanding and broadens the possible application of the Zak phase in a non-Hermitian system.

DOI: 10.1103/PhysRevA.99.012113

I. INTRODUCTION

The scope of quantum mechanics has been extended to a non-Hermitian system since the discovery that a certain class of non-Hermitian Hamiltonians could exhibit the entirely real spectra [1–3] and the observation of non-Hermitian behavior in experiment [4–12]. Besides the exceptional point (EP), a biorthonormal inner product can be induced to take the role of the Dirac inner product for a pseudo-Hermitian Hamiltonian operator [13,14], which always associates with a particular symmetry, $\mathcal{PT}$ symmetry. Here $\mathcal{P}$ is an unitary operator, while $\mathcal{T}$ is an antiunitary operator. Especially in the $\mathcal{PT}$ symmetric region, a non-Hermitian Hamiltonian acts as a Hermitian one, having entirely real spectrum, unitary evolution, etc., in the context of biorthonormal inner product. In this sense, many conclusions for Hermitian system can be extended to the non-Hermitian regime. Recently there has been a growing interest in topological properties of non-Hermitian Hamiltonians applicable to a wide range of systems including systems with unbalanced pairing, systems with gain and/or loss and systems with open boundaries [15–31]. In this area, theoretical studies of non-Hermitian topological systems usually focus on either concrete experimental realizations of dissipative topological in real material or finding topological invariants or systematic classification of topological phases [23,32–40].

In the Hermitian regime, it is well known that the nontrivial band topologies of both two-dimensional (2D) and 3D systems are characterized by the Chern numbers and the Z_2 invariants, respectively, while the topological property of bulk bands in 1D periodic systems is characterized by the Zak phase [41]. However, the role of the Zak phase is subtle: The Zak phase is not a geometric invariant, since it depends on the choice of origin of the Brillouin zone. Only the Zak phase difference can identify a topological transition. On the other hand, it has been shown that the geometric phase can be complex [42–50] in a non-Hermitian system. Motivated by the performance of the Zak phase in a non-Hermitian system, in this work, we investigate the influence of non-Hermitian term on the Zak phase in a bipartite lattice.

If a Hermitian system is topological, then a natural question to ask is how does the non-Hermitian term can effect on the topology of the original Hermitian system. In general, there exists three possibilities: (i) The system possesses the original topology even in the presence of the non-Hermitian term. (ii) The system remains partial topology of its original one. (iii) The existence of the non-Hermitian term spoils the original topology. Which one does the non-Hermitian system prefer? This is what we need to answer in this paper. Through the analytical solution, we find that when the staggered on-site potential is added, a class of non-Hermitian bipartite systems can still inherit partially the topology of the original Hermitian systems through the real part of Zak phase. The non-Hermitian term only brings about an imaginary part of Zak phase. Such a complex quantity has physical implication

*songtc@nankai.edu.cn

when we relate it to a complex Berry phase through adiabatic evolution of a time-dependent Hamiltonian driven by the magnetic flux. In this context, we point out that the Zak phase difference between different parameter regions can be dynamically characterized by the scattering of a wave packet. Due to the partial topology of Zak phase, the wave packets after the interference will exhibit the partial confinement behavior. This also provide a possible experimental scheme to observe the topological invariants.

This paper is organized as follows. In Sec. II, we present a general theory about the partial topological phase in a 1D non-Hermitian bipartite system. In Sec. III, we apply the theory to a concrete model and provide a dynamical method to realize the Zak phase. Section IV devotes to the scattering behaviors based on the topological feature of the Zak phase. Finally, we give a summary and discussion in Sec. V.

II. ZAK PHASE IN A NON-HERMITIAN BIPARTITE SYSTEM

We first investigate the generic non-Hermitian lattice models that consist of two sublattices, A and B, the non-Hermiticity of which stems from the staggered imaginary on-site potential. For clarity, we start discussion with systems that possess the identical sublattice numbers $A = B = N$. The corresponding bipartite non-Hermitian Hamiltonian can be written as

$$\mathcal{H} = \sum_{ij} w_{ij} c^{\dagger}_{A,i} c_{B,j} + \text{H.c.} - i\Delta \sum_{i} (c^{\dagger}_{A,i} c_{A,i} - c^{\dagger}_{B,i} c_{B,i}), \tag{1}$$

where $c^{\dagger}_{A(B),j}$ denotes the creation operator of an electron on site A (B) with periodic boundary condition $c^{\dagger}_{A(B),j} = c^{\dagger}_{A(B),j+N}$ and w_{ij} is a complex number describing the coupling constant between the two sublattices. A schematic illustration of the model is presented in Fig. 1. Due to the complexity of the coupling w_{ij}, the system does not have the chirality-time-reversal symmetry but has translation

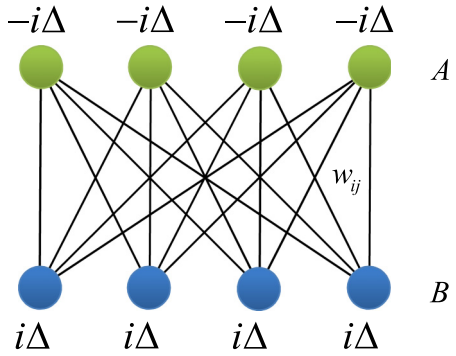

FIG. 1. Schematic illustration of the non-Hermitian bipartite lattice that consists of two sublattices A and B with identical lattice length. The two sublattices are connected with each other by bond w_{ij} which is across the ith site in sublattice A and the jth site in sublattice B.

symmetry with the condition $w_{ij} = w_{i+1,j+1}$, i.e., $[T, \mathcal{H}] = 0$. Here the translation operator T is defined as

$$T^{-1} c^{\dagger}_{A(B),j} T = c^{\dagger}_{A(B),j+1}, \tag{2}$$

which allows the invariant subspace spanned by the eigenvector of operator T. Taking the Fourier transformation, the non-Hermitian Bloch Hamiltonian of a lattice with translational symmetry then reads $\mathcal{H} = \sum_k H_k$, satisfying $[H_{k'}, H_k] = 0$. In the Nambu representation, the bipartite non-Hermitian Hamiltonian can be written as

$$\mathcal{H} = \sum_k \eta^{\dagger}_k h_k \eta_k, \tag{3}$$

where the basis $\eta^{\dagger}_k = (c^{\dagger}_{A,k}, c^{\dagger}_{B,k})$ with $c^{\dagger}_{A(B),k}$ the creation operator of a Fermion in the momentum space, which satisfies $T^{-1} c^{\dagger}_{A(B),k} T = e^{-ik}$, and

$$h_k = \vec{B}(k) \cdot \vec{\sigma}, \tag{4}$$

with $\vec{\sigma} = (\sigma_x, \sigma_y, \sigma_z)$ the vector of the matrices. Note that $\vec{B}(k) = [B_x(k), B_y(k), B_z]$ is a three-dimensional complex vector field, where $B_z = -i\Delta$ is k independent. The presence of the staggered imaginary on-site potential results in the imaginary strength of z direction of $\vec{B}(k)$, i.e., $B^*_z = -B_z$. The general energy expression of the single quasiparticle can be given as $\varepsilon_k = \pm r_k$, where $r_k = \sqrt{B^2_x(k) + B^2_y(k) - [\text{Im}(B_z)]^2}$. It is clear that when any one of the quasimomenta k satisfies $B^2_x(k) + B^2_y(k) - [(\text{Im}(B_z)]^2 < 0$, the imaginary energy level appears in the quasiparticle spectrum, which leads to the occurrence of complex energy levels. This result has three implications. (i) The non-Hermitian Hamiltonian $\mathcal{H}$ is pseudo-Hermitian, since its eigenvalues are either real or come in complex-conjugate pairs. (ii) One can always modulate the strength of imaginary on-site potential to obtain the full real spectrum. The critical strength of the imaginary on-site potential depends on the energy gap between the two bands of the Hermitian version with $B_z = 0$. (iii) The EP occur at $B^2_x(k) + B^2_y(k) = [\text{Im}(B_z)]^2$, which corresponds to the Jordan Block of h_k accompanied by the coalescence of the two eigenstates. Now we give the expression of the eigenstates. The eigenstates of a bipartite non-Hermitian Hamiltonian can construct a complete set of biorthogonal bases in association with the eigenstates of its Hermitian conjugate. For the concerned bipartite system, $|\varrho^k_+\rangle$, $|\varrho^k_-\rangle$ of h_k and $|\chi^k_+\rangle$, $|\chi^k_-\rangle$ of $h^{\dagger}_k$ are the biorthogonal bases of the single-quasiparticle invariant subspace, which are explicitly expressed as

$$|\varrho^k_+\rangle = \begin{pmatrix} \cos\frac{\theta}{2} e^{-i\varphi} \\ \sin\frac{\theta}{2} \end{pmatrix}, \quad |\varrho^k_-\rangle = \begin{pmatrix} \sin\frac{\theta}{2} \\ -\cos\frac{\theta}{2} e^{i\varphi} \end{pmatrix}, \tag{5}$$

$$|\chi^k_+\rangle = \begin{pmatrix} \cos\frac{\theta}{2} e^{i\varphi} \\ \sin\frac{\theta}{2} \end{pmatrix}^*, \quad |\chi^k_-\rangle = \begin{pmatrix} \sin\frac{\theta}{2} \\ -\cos\frac{\theta}{2} e^{-i\varphi} \end{pmatrix}^*. \tag{6}$$

Here the vector field $\vec{B}(k)$ is represented in terms of polar coordinates as

$$\vec{B}(k) = r_k(\sin\theta\cos\varphi, \sin\theta\sin\varphi, \cos\theta), \tag{7}$$

where

$$r_k = \sqrt{B_x^2(k) + B_y^2(k) - [\mathrm{Im}(B_z)]^2}, \tag{8}$$

$$\cos\theta = \frac{B_z}{r_k}, \ \tan\varphi = \frac{B_y(k)}{B_x(k)}. \tag{9}$$

It is easy to check that biorthogonal bases $\{|\varrho_\lambda^k\rangle, |\chi_\lambda^k\rangle\}(\lambda = \pm)$ satisfy the biorthogonal and completeness conditions,

$$\langle\varrho_\lambda^k|\chi_{\lambda'}^{k'}\rangle = \delta_{\lambda\lambda'}\delta_{kk'}, \ \sum_{\lambda k}|\varrho_\lambda^k\rangle\langle\chi_\lambda^k| = I. \tag{10}$$

Note that these properties are independent of the reality of the spectrum and are generally satisfied except at the EP. In the absence of the staggered imaginary on-site potential, we have $|\varrho_\lambda^k\rangle = |\chi_\lambda^k\rangle$ with $\theta = \pi/2$ and the conditions (10) reduce to the Dirac orthogonal and completeness conditions. In the following, we focus on the system with full real spectrum. This is crucial to achieve the main conclusion. To characterize the topological property of the energy band, we introduce the modified Zak phase

$$\mathcal{Z}_\pm = \int_0^{2\pi} \mathcal{A}_{k,\pm}dk, \tag{11}$$

where the Berry connection is given by

$$\mathcal{A}_{k,\pm} = i\langle\chi_\pm^k|\partial_k|\varrho_\pm^k\rangle = \partial_k\varphi\mathcal{A}_{\varphi,\pm} + \partial_k\theta\mathcal{A}_{\theta,\pm}, \tag{12}$$

with

$$\mathcal{A}_{\varphi,\pm} = i\langle\chi_\pm^k|\partial_\varphi|\varrho_\pm^k\rangle, \ \mathcal{A}_{\theta,\pm} = i\langle\chi_\pm^k|\partial_\theta|\varrho_\pm^k\rangle. \tag{13}$$

The straightforward algebra shows that

$$\mathcal{Z}_\pm = \pm\frac{1}{2}\int_{\varphi(0)}^{\varphi(2\pi)}(1+\cos\theta)d\varphi, \tag{14}$$

$$= Z_\pm \pm i\frac{\mathrm{Im}(B_z)}{2}\int_{\varphi(0)}^{\varphi(2\pi)}\frac{1}{r_k}d\varphi, \tag{15}$$

where Z denotes the Zak phase of the Hermitian system without staggered imaginary potential, i.e., the Bloch Hamiltonian h_k with $\vec{B}(k) = (B_x(k), B_y(k), 0)$. Comparing to the Hermitian version with $\theta = \pi/2$, the presence of the staggered imaginary potential does not alter the real part of the Zak phase but brings about an extra imaginary part, which amplifies the Dirac probability of the adiabatic evolved state. In this sense, if the Zak phase of the original Hermitian bipartite Hamiltonian is topological, then the modified Zak phase of the non-Hermitian version will inherit this topological property through its real part. Such a modified Zak phase is therefore referred to as the partial topological Zak phase.

A. Two concrete bipartite non-Hermition models

Here we want to point out that this conclusion is held for a class of non-Hermitian bipartite lattice models. To demonstrate this finding, we consider two concrete models, the non-Hermitian Su-Schrieffer-Heeger (SSH) model and the coupled SSH model, which are shown in Fig. 2.

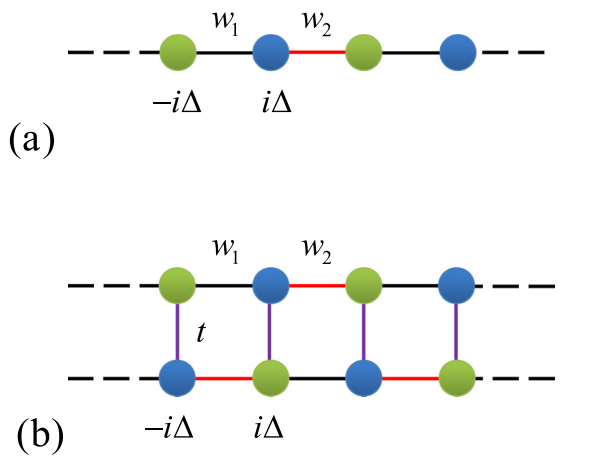

FIG. 2. Schematic illustration of two typical bipartite non-Hermitian lattice systems: (a) a non-Hermitian SSH model with staggered on-site imaginary potential and (b) a non-Hermitian coupled SSH model. It consists of two non-Hermitian SSH chains with periodical boundary condition. The non-Hermitian systems inherit the topology of the original Hermitian system through the real part of a Zak phase.

1. Non-Hermitian SSH model

For a non-Hermitian SSH model, the Hamiltonian can be given as

$$\mathcal{H} = \sum_j w_1 c_{A,j}^\dagger c_{B,j} + w_2 c_{B,j}^\dagger c_{A,j+1} + \mathrm{H.c.} - i\Delta\sum_j(c_{A,j}^\dagger c_{A,j} - c_{B,j}^\dagger c_{B,j}), \tag{16}$$

where w_i $(i = 1, 2)$ is a positive real number and describes the staggerd hopping amplitude. Applying the Fourier transformation

$$c_{A,k}^\dagger = \frac{1}{\sqrt{N}}\sum_j e^{ik}c_{A,j}^\dagger, \tag{17}$$

$$c_{B,k}^\dagger = \frac{1}{\sqrt{N}}\sum_j e^{ikj}c_{B,j}^\dagger, \tag{18}$$

one can immediately obtain the vector field $\vec{B}(k)$ as

$$B_x(k) = w_1 + w_2\cos k, \tag{19}$$

$$B_y(k) = w_2\sin k, \tag{20}$$

$$B_z = -i\Delta. \tag{21}$$

Substituting the expressions (19)–(21) into Eq. (14), the corresponding Zak phase is

$$\mathcal{Z}_\pm = \left[Z_\pm \mp i\Delta\int_{\varphi(0)}^{\varphi(2\pi)}\frac{1}{r_k}d\varphi\right], \tag{22}$$

with

$$Z_\pm = \begin{cases}\pi, & w_2 > w_1\\ 0, & \text{otherwise}\end{cases}. \tag{23}$$

Obviously, the real part of the Zak phase is topological. This can be also understood with the help of the auxiliary $B_x - B_y$ space. In that sapce, $B_x(k)$ and $B_y(k)$ form a loop as k changes from 0 to π. Evidently, the real part of the Zak phase characterizes the winding number of the loop around the origin of the $B_x - B_y$ space. Note that the Zak phase is not a topological invariant, since it depends on the choice of origin of the Brillouin zone. Specifically, one can change the value of Zak phase through the different Fourier transformations, which will be demonstrated in Sec. III.

2. Non-Hermitian coupled SSH model

The coupled SSH model consists of two SSH chains with a periodical boundary condition. The geometry of this system is illustrated in Fig. 2(b), in which the hopping amplitudes and on-site potential in each leg are staggered. Such a ladder system is a bipartite lattice system, consisting of two sublattices A and B. We write down the Hamiltonian for the system in a simple form,

$$\mathcal{H} = \sum_j w_1 c^\dagger_{A,j} c_{B,j+1} + w_2 c^\dagger_{B,j} c_{A,j+1} + t c^\dagger_{A,j} c_{B,j} + \text{H.c.} - i\Delta \sum_j (c^\dagger_{A,j} c_{A,j} - c^\dagger_{B,j} c_{B,j}), \tag{24}$$

where t depicts the coupling between the two legs. With the same procedures, we can obtain the complex vector field $\vec{B}(k)$ with

$$B_x(k) = (w_1 + w_2)\cos k + t, \tag{25}$$

$$B_y(k) = (w_2 - w_2)\sin k, \tag{26}$$

$$B_z = -i\Delta. \tag{27}$$

Following the idea in the previous subsection, it represents an ellipse with the center located at $(t,\ 0)$ in the auxiliary $B_x - B_y$ space. Therefore we can infer that the real part of the Zak phase is topological: When $|t| > |w_1 + w_2|$, the origin is out of the ellipse, resulting zero real part of Zak phase. Otherwise, the real part of Zak phase is $\pm\pi$ depending on the direction of the loop when k increases from 0 to 2π . With this spirit, the Zak phase can be given as

$$\mathcal{Z}_\pm = \pm \begin{cases} 0 + i\Gamma, & |t| > |w_1 + w_2| \\ \pi\,\text{sgn}\left(w_2^2 - w_1^2\right) + i\Gamma, & \text{otherwise} \end{cases}, \tag{28}$$

where sgn(.) denotes the sign function and

$$\Gamma = -i\frac{\Delta}{2}\int_{\varphi(0)}^{\varphi(2\pi)} \frac{1}{r_k} d\varphi. \tag{29}$$

In the following section, we will demonstrate first the partial topological Zak phase can be realized by a magnetic-flux-driven non-Hermitian SSH ring and then apply it to a scattering problem.

III. NON-HERMITIAN SSH MODEL WITH FLUX

We consider a bipartite non-Hermitian SSH ring threaded by magnetic flux, the Hamiltonian of which can be given as

$$H = -\frac{1}{2}\sum_{j=1}^{2N}[1 + (-1)^j\delta](e^{i\phi}c^\dagger_j c_{j+1} + \text{H.c.}) + i\Delta\sum_j (-1)^j c^\dagger_j c_j, \tag{30}$$

the non-Hermiticity of which arises from the on-site staggered imaginary potential $i\Delta\sum_j (-1)^j c^\dagger_j c_j$. The system possesses a $2N$-site lattice, where c_j is the annihilation operator on site j with the periodic boundary condition $c_{j+2N} = c_j$. The nominal tunneling strength is staggered by δ, and $\Phi = 2N\phi$ is the magnetic flux threading the ring. We sketch the structure of the system in Fig. 3. The original Hermitian Hamiltonian with $\Delta = 0$ can be realized with controlled defects using a system of attractive ultracold fermions [51–53] in a simple shaken one-dimensional optical lattice. Furthermore, the non-Hermitian version can be realized in a zigzag array of optical waveguides with alternating optical gain and loss [54]. Before solving the Hamiltonian, it is profitable to investigate the symmetry of the system and its breaking in the eigenstates. Straightforward algebra shows that $[\mathcal{PT}, H] = 0$, that is, the Hamiltonian is $\mathcal{PT}$ symmetric even in the presence of the magnetic flux, where the antilinear time-reversal operator $\mathcal{T}$ has the function $\mathcal{T}^{-1}i\mathcal{T} = -i$ and the parity operator obeys $\mathcal{P}^{-1}c^\dagger_j\mathcal{P} = c^\dagger_{2N-j+1}$. However, the eigenstates does not always hold this symmetry. According to the non-Hermitian quantum mechanics, the occurrence of the EP always accomplishes the $\mathcal{PT}$ symmetry breaking of an eigenstate. In the following, we will demonstrate this point.

We note that the Hamiltonian is invariant through a translational transformation, i.e., $[T, H] = 0$, where T is the shift operator that defined as

$$T^{-1}c^\dagger_j T = c^\dagger_{j+2}. \tag{31}$$

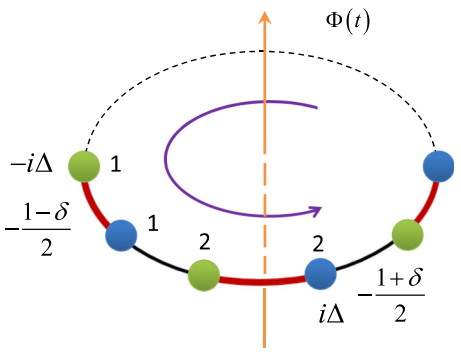

FIG. 3. Schematic illustration of the non-Hermitian SSH model driven by a time-dependent external field. The presence of the magnetic field does not spoil the $\mathcal{PT}$ symmetry of the system. A time-varying field $\Phi(t)$ induces the eddy field in a direction indicated by the purple arrow, which acts as a linear field to drive the wave-packet dynamics.

This allows invariant subspace spanned by the eigenvector of operator T. The single-particle eigenvector of T_2 can be expressed as $c^\dagger_{A,k}|0\rangle$ and $c^\dagger_{B,k}|0\rangle$, where

$$c^\dagger_{A,k} = \frac{1}{\sqrt{N}}\sum_j e^{ik(j-1/2)}c^\dagger_{2j-1}, \tag{32}$$

$$c^\dagger_{B,k} = \frac{1}{\sqrt{N}}\sum_j e^{ikj}c^\dagger_{2j}, \tag{33}$$

satisfying

$$T^{-1}c^\dagger_{A(B),k}T = e^{-ik}c^\dagger_{A(B),k}. \tag{34}$$

Here $c^\dagger_{A,k}$ and $c^\dagger_{B,k}$ are two kinds of creation operators of bosons (or fermions), with $k = 2\pi n/N$ ($n \in [1, N]$), representing the particles in odd and even sublattices. Then the Bloch Hamiltonian H_k can be given as $H_k = \eta^\dagger_k h_k \eta_k$, where $h_k = \overrightarrow{B}(k)\cdot\overrightarrow{\sigma}$ with the 3D vector field

$$B_x(k) = -\cos(k/2+\phi), \tag{35}$$

$$B_y(k) = -\delta\sin(k/2+\phi), \tag{36}$$

$$B_z = -i\Delta. \tag{37}$$

Accordingly, the eigenvalue of single quasiparticle can be obtain readily as

$$\varepsilon_k = \pm r_k, \tag{38}$$

$$r_k = \sqrt{\cos^2(k/2+\phi) + \delta^2\sin^2(k/2+\phi) - \Delta^2}. \tag{39}$$

Here we want to point out that in the absence of Δ, the energy gap is 2δ, which determines the EP occurring at $\Delta = \Delta_c = \delta$. The corresponding biorthogonal eigenstates can be determined by Eqs. (5) and (6), which can be expressed as

$$|\varrho^k_+\rangle = \cos\frac{\theta}{2}e^{-i\varphi}c^\dagger_{A,k}|\mathrm{Vac}\rangle + \sin\frac{\theta}{2}c^\dagger_{B,k}|\mathrm{Vac}\rangle, \tag{40}$$

$$|\varrho^k_-\rangle = \sin\frac{\theta}{2}c^\dagger_{A,k}|\mathrm{Vac}\rangle - \cos\frac{\theta}{2}e^{i\varphi}c^\dagger_{B,k}|\mathrm{Vac}\rangle, \tag{41}$$

where $|\mathrm{Vac}\rangle$ is the vacuum state of the fermion c_j, and

$$\cos\theta = \frac{-i\Delta}{r_k},\quad \tan\varphi = \frac{\delta\sin(k/2+\phi)}{\cos(k/2+\phi)}. \tag{42}$$

Applying the $\mathcal{PT}$ operator to the fermion operators and its vacuum state $|\mathrm{Vac}\rangle$, we have

$$(\mathcal{PT})^{-1}c^\dagger_{A(B),k}\mathcal{PT} = e^{-ik/2}c^\dagger_{B(A),k} \tag{43}$$

and

$$\mathcal{PT}|\mathrm{Vac}\rangle = 0, \tag{44}$$

which are available in both the broken and unbroken region. Due to the relation $[\mathcal{PT}, H] = 0$, the eigenstate $|\varrho^k_\lambda\rangle$ of H for a real eigenvalue is always the eigenstate of the symmetry operator $\mathcal{PT}$, that is, $\mathcal{PT}|\varrho^k_\pm\rangle = \pm e^{\pm i\varphi}|\varrho^k_\pm\rangle$. However, when the system is in the spontaneously broken $\mathcal{PT}$-symmetric phase ($\varepsilon^*_k = -\varepsilon_k$), the coefficients $\cos\frac{\theta}{2}$ and $\sin\frac{\theta}{2}$ experience a transition as

$$\left(\cos\frac{\theta}{2}\right)^* = \cos\frac{\theta}{2}, \tag{45}$$

$$\left(\sin\frac{\theta}{2}\right)^* = -\sin\frac{\theta}{2}, \tag{46}$$

which directly leads to $\mathcal{PT}|\varrho^k_\pm\rangle = -|\varrho^k_\mp\rangle$. Therefore, the eigenstate $|\varrho^k_\lambda\rangle$ is not $\mathcal{PT}$ symmetric.

With the help of Eq. (14), one can give directly the modified Zak phase based on the analytical solution

$$\mathcal{Z}_\pm = \pm\left[\frac{\pi\,\mathrm{sgn}(\delta)}{2} - i\Delta\delta\int_0^{2\pi}\frac{1}{4r_k\left(r_k^2+\Delta^2\right)}dk\right], \tag{47}$$

Note that we only consider the case of the system with a full real spectrum. There are two features in the expression of $\mathcal{Z}_\pm$: (i) $\mathcal{Z}_\pm$ does not depend on the magnetic flux ϕ due to the relation $\mathcal{A}_{k,\lambda} = \mathcal{A}_{k+2\pi,\lambda}$. (ii) The real part of $\mathcal{Z}_\pm$ is topological. Here we want to stress that the real part of $\mathcal{Z}_\pm$ is not gauge invariant since the different Fourier transformations can change its value, which can be seen from the Eq. (22). However, the difference of real part between $\mathcal{Z}_\pm$ in the regions of $\delta > 0$ and $\delta < 0$ is gauge invariance. Therefore the Zak phase difference can be utilized to identify a topological transition. This property also provides a way to adiabatically control the scattering of the wave-packet dynamics in the following section.

Before starting the discussion of the wave-packet dynamics, we first connect the magnetic-flux-driven Berry phase to the modified Zak phase $\mathcal{Z}_\pm$. To this end, we consider an adiabatic evolution, in which an initial eigenstate evolves into the instantaneous eigenstate of the time-dependent Hamiltonian. From Eq. (30), we know that H is a periodic function of ϕ, $H(\phi) = H(\phi + 2\pi)$. Considering the time-dependent flux $\phi(t)$, any eigenstate $|\varrho^k_\lambda(0)\rangle$ will return back to $|\varrho^k_\lambda(0)\rangle$ if $\phi(t)$ varies adiabatically from 0 to 2π, and the evolved state is the instantaneous eigenstate $|\varrho^k_\lambda(\phi)\rangle$. More explicitly, the adiabatic evolution of the initial eigenstate $|\varrho^k_\lambda(0)\rangle$ under the time-dependent Hamiltonian $H(\phi(t))$ can be expressed as

$$\begin{aligned}\left|\Psi^k_\lambda(\phi)\right\rangle &= \mathcal{T}\exp\left[-i\int_0^t H(t)dt\right]\left|\varrho^k_\lambda(0)\right\rangle \\ &= e^{i\left(\alpha^\lambda_k+\gamma^\lambda_k\right)}\left|\varrho^k_\lambda(\phi)\right\rangle.\end{aligned} \tag{48}$$

Here $\alpha^\lambda_k(\phi)$ the dynamics phase and $\gamma^\lambda_k(\phi)$ the adiabatic phase have the form

$$\alpha^\lambda_k(\phi) = -\int_0^\phi \varepsilon^k_\lambda(\phi)\frac{\partial t}{\partial\phi}d\phi, \tag{49}$$

$$\gamma^\lambda_k(\phi) = \lambda\int_0^\phi \mathcal{A}_\phi d\phi, \tag{50}$$

where the Berry connection $\mathcal{A}_\phi = \delta/2r_k(r_k + i\Delta)$ with $\mathcal{A}_\phi = \mathcal{A}_{\phi+\pi}$. When the flux ϕ varies from 0 to π, one can verify that the adiabatic phase is k independent, which is similar to the case in the modified Zak phase. Correspondingly, the

expression of adiabatic phase can be given as

$$\gamma^{\pm} = \pm\left[\frac{\pi\,\mathrm{sgn}(\delta)}{2} - i\,\Delta\delta\int_0^{\pi}\frac{1}{2r_k\left(r_k^2+\Delta^2\right)}d\phi\right]. \quad (51)$$

For a Hermitian system, the adiabatic phase is always real that ensures the probability preserving evolution, while the probability of an evolved state changes due to the imaginary part of the adiabatic phase in a non-Hermitian system. The attenuation or amplification of probability depends on the sign of the imaginary phase. Straightforward algebra shows that the imaginary part of $\mathcal{Z}_{\pm}$ is the same as the imaginary part of $\gamma^{\pm}$. This is always true for any values of k (ϕ) for $\mathcal{Z}_{\pm}$ ($\gamma^{\pm}$). In this sense, one can mimic the modified Zak phase $\mathcal{Z}_{\pm}$ through the adiabatic variation of magnetic flux from 0 to π. Here we want to point out that although the magnetic-flux-driven adiabatic phase is identical to the modified Zak phase, the evolve state $|\Psi_{\lambda}^{k}(\pi)\rangle$ does not return back to the initial state. One can readily obtain the $|\Psi_{\lambda}^{k}(\pi)\rangle$ by modulating $\varphi \to \varphi + \pi$ in initial state $|\varrho_{\lambda}^{k}(0)\rangle$. In the coordinate space, it can be achieved through modulating π phase of the distribution on the odd site, that is,

$$\begin{aligned}\left|\Psi_{\lambda}^{k}(\pi)\right\rangle &= e^{i\alpha_k^{\lambda}(\pi)}e^{i\gamma^{\lambda}}\left|\varrho_{\lambda}^{k}(\pi)\right\rangle,\\ &= \frac{e^{i\alpha_k^{\lambda}(\pi)}e^{i\gamma^{\lambda}}}{\sqrt{N}}\sum_j\left[-\cos\frac{\theta}{2}e^{-i\varphi}e^{ik(j-1/2)}c_{2j-1}^{\dagger}\right.\\ &\quad\left.+\sin\frac{\theta}{2}e^{ikj}c_{2j}^{\dagger}|\mathrm{Vac}\rangle\right]. \quad (52)\end{aligned}$$

This is crucial step to understand the wave-packet dynamics in the following.

Now switch gear to the adiabatic time evolution of the wave packet. We consider two kinds of functions $\phi(t)$. For the first one, the magnetic flux ϕ linearly depends on time, that is, $\phi = \beta t$. When the flux ϕ varies from 0 to π, the dynamics phase $\alpha_k^{\lambda}(\pi)$ is k independent, which can be verified through the fact that $\varepsilon_k(\phi) = \varepsilon_k(\phi+\pi)$. Therefore, if one considers the wave-packet dynamics, the adiabatic phase and dynamics phase are served as an overall phase and cannot induce the interference among the instantaneous eigenstates. More explicitly, we consider the wave packet localized on the upper band of the system (the conclusion is also hold for the case of lower band),

$$\left|G_{k_0}^{N_A}(0)\right\rangle = \sum_k g_k\left|\varrho_{+}^{k}(0)\right\rangle, \quad (53)$$

where N_A and k_0 denote the center and velocity of the initial wave packet, respectively. Here we do not give the explicit expression of the coefficient g_k, since the following analysis is irrelevant to g_k. In the coordinate space, the wave packet can be expressed as

$$|G(0)\rangle = \sum_j f_j c_j^{\dagger}|\mathrm{Vac}\rangle, \quad (54)$$

where the scripts N_A and k_0 are neglected. Through an adiabatic evolution in which ϕ varies from 0 to π, the adiabatic phase and dynamics phase is an overall phase and then we have

$$|G(\pi)\rangle = e^{i\Omega_+}e^{\xi_+}\sum_k g_k|\varrho_{+}^{k}(\pi)\rangle, \quad (55)$$

where $\Omega_+ = \alpha^+(\pi) + \mathrm{Re}(\gamma^+)$ and $\xi_+ = -\mathrm{Im}(\gamma^+)$. Due to the relation (52), the evolved wave packet at time $t = \pi/\beta$ in the coordinate space can be given as

$$|G(\pi)\rangle = e^{i\Omega_+}e^{\xi_+}\sum_j(-1)^j f_j c_j^{\dagger}|\mathrm{Vac}\rangle, \quad (56)$$

where the odd site acquires a phase π. It indicates that the two wave packets $|G(0)\rangle$ and $|G(\pi)\rangle$ are orthogonal based on

$$\mathcal{F}(\pi) = \frac{\langle G(0)|\,G(\pi)\rangle}{\sqrt{\langle G(0)|\,G(0)\rangle\langle G(\pi)|\,G(\pi)\rangle}} = 0. \quad (57)$$

To demonstrate this feature, we plot the trajectories of the wave packet with different β in Figs. 4(a)–4(c). It can be shown that the wave packet experiences half a Bloch oscillation (BO) accompanied by the probability amplification in the coordinate space. The dynamics of a wave packet driven by time-dependent magnetic flux is the same as that driven by a linear field with strength β, according to the quantum Faraday's law [55]. Furthermore, the center path of a wave packet driven by a linear field accords with the dispersion of the Hamiltonian in the absence of the field within the adiabatic regime [56],

$$x_c(\phi) = x_c(0) + \frac{1}{\beta}\left[\varepsilon_{k_c}(\phi) - \varepsilon_{k_c}(0)\right], \quad (58)$$

where $\varepsilon_{k_c}(\phi)$ is the dispersion relation and k_c is the central momentum of the wave packet. From this perspective, the amplitude of the BO of the wave packet is inversely proportional to β.

For the second one, the magnetic flux varies with time according to the error function curve, that is, $\phi = \mathrm{erf}(t)$, where erf(.) is the error function. In this situation, the dynamics phase $\alpha_k^{\lambda}(\pi)$ is k dependent but the adiabatic phase $\gamma^{\pm}$ is still k independent. Therefore the dynamics of the wave packet is more complicated than the case of $\phi = \beta t$. In Fig. 5, we plot the trajectory of the wave packet. On the one hand, we can see that when $d\phi/dt$ is small, which corresponds to two ends of the error function, the wave packet travels at approximately uniform speed. In this condition, the effective linear field with strength β is approximate zero. On the other hand, the derivative $d\phi/\mathrm{dt}$ is linear in the middle of the error function. Therefore, there exists a linear field that drives the wave-packet oscillate in the coordinate space, which can be shown in Fig. 5. For the sake of simplicity, we consider the first case where $\phi = \beta t$ to realize the dynamical control of the wave packet.

IV. TRANSMISSION AND CONFINEMENT

In this section, we will control the scattering behavior of the wave packet based on the partial topological property of the Zak phase. We will show that the wave packet will display two distinct dynamical behaviors in the modulating non-Hermitian scattering network, that is, perfect transmission and partial confinement.

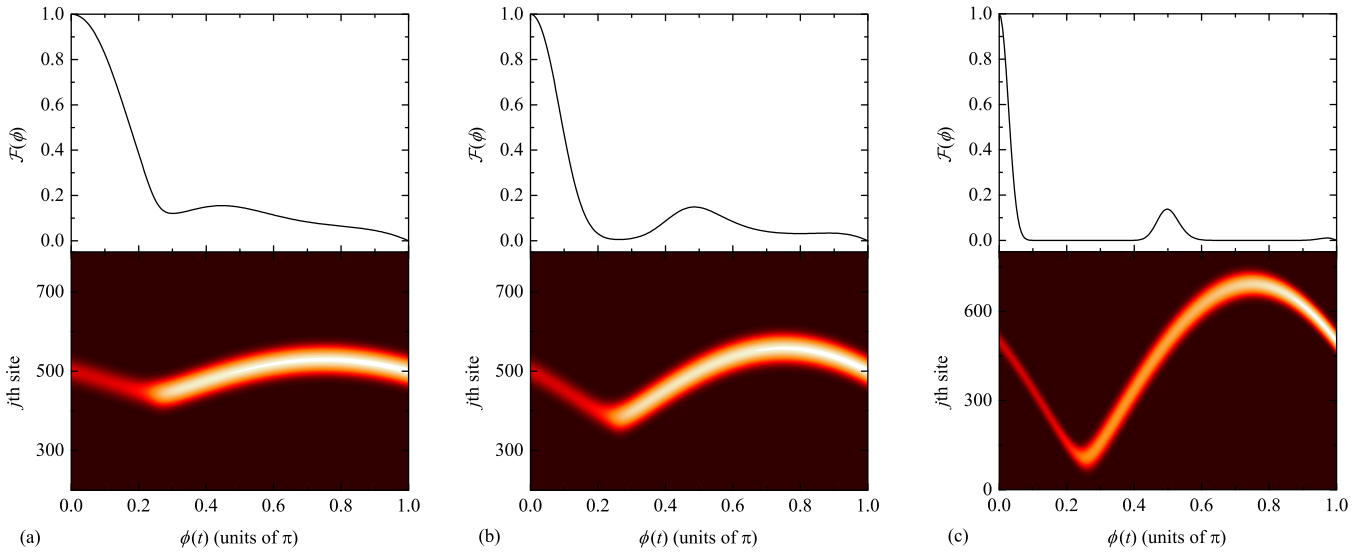

FIG. 4. The profiles of the time evolution of a wave packet in several typical cases. The initial wave packet is in the form of Eq. (53) with $g_k = \exp[-(k-k_0)^2/4\alpha^2 - i(k-k_c)N_c]$, where the half width of the wave packet $\alpha = 0.05$, central momentum $k_0 = \pi/4$, and the location of the initial state $N_c = 250$. The time is in units of J^{-1}, where J is the scale of the Hamiltonian and we take $J = 1$. The other system parameters are $\delta = 0.15$ and $\Delta = 0.1$. The magnetic flux adiabatically varies with (a) $\beta = 0.01$, (b) $\beta = 0.005$, and (c) $\beta = 0.0015$, respectively. It can be shown that the wave packet exhibits half a BO with different amplitude which is determined by β. After half a BO, the wave packet return back to the starting position. However, it is orthogonal to the initial state that can be shown in the upper panel of each subfigures. The numerical results demonstrate our analytical statement below Eq. (58).

A. Interferometer

In order to demonstrate these behaviors, we first consider the interferometer model which is illustrated schematically in Fig. 6. This quantum interferometer consists of two non-Hermitian SSH chains A, D and a ring $\{B_1, B_2\}$ threaded by magnetic flux in the unit of flux quanta. The corresponding Hamiltonian reads

$$H_{\rm net} = -\frac{1}{2}\sum_{\alpha}(H_\alpha + H_{\rm joint}), \tag{59}$$

where $\alpha = A,\ B_1,\ B_2,\ D$ denote four non-Hermitian SSH chains, respectively, and

$$H_{\sigma_1} = \sum_{j=1}^{2N_{\sigma_1}-1}[1+(-1)^j\delta]\left(c^\dagger_{\sigma_1,j}c_{\sigma_1,j+1} + \text{H.c.}\right) - 2i\Delta\sum_{j=1}^{2N_{\sigma_1}-1}(-1)^j c^\dagger_{\sigma_1,j}c_{\sigma_1,j}, \tag{60}$$

$$H_{\sigma_2} = \sum_{j=1}^{2N_{\sigma_2}-1}[1+(-1)^j\delta]\left(e^{i\phi}c^\dagger_{\sigma_2,j}c_{\sigma_2,j+1} + \text{H.c.}\right) - 2i\Delta\sum_{j=1}^{2N_{\sigma_2}-1}(-1)^j c^\dagger_{\sigma_1,j}c_{\sigma_1,j}, \tag{61}$$

where $\sigma_1 = A,\ D$ and $\sigma_2 = B_1,\ B_2$. Note that H_{B_1} and H_{B_2} describe the two identical non-Hermitian SSH chains with length $N_B \equiv N_{B_1} = N_{B_2}$. The connection Hamiltonian reads

$$H_{\rm joint} = \frac{(1+\delta)}{\sqrt{2}}\left(e^{i\phi}c^\dagger_{A,2N_A,}c_{B_1,1} + e^{-i\phi}c^\dagger_{A,2N_A,}c_{B_2,1} + e^{i\phi}c^\dagger_{B_1,2N_B,}c_{D,1} + e^{-i\phi}c^\dagger_{B_2,2N_B,}c_{D,1} + \text{H.c.}\right). \tag{62}$$

Here $\Phi = 4(N_B + 1/2)\phi$ is the total magnetic flux threading the ring. Now we focus on the dynamics of the wave packet based on the partial topological property of the modified Zak phase. To this end, we take the initial state as the Gaussian wave packet (GWP)

$$|G(k_0,0)\rangle = \frac{1}{\sqrt{\Omega}}\sum_{l=1}^{2N_A} e^{-\alpha^2(l-N_c)^2}e^{ik_0 l}c^\dagger_{A,l}|\text{Vac}\rangle, \tag{63}$$

with the central momentum k_0. Here Ω is the normalization factor and $N_c \in [1, 2N_A]$ is the initial central position of the GWP at the input chain A while the factor α is large enough to guarantee the locality of the state in the chain A. According to the Ref. [57], when the center momentum k_0 satisfies the condition $|k_0 + \pi/2| \gg 0$ and δ is a small number, the initial state will distribute on $k \sim 2k_0$ in the upper band of the Hamiltonian H_A with a periodic boundary condition. It is worthy pointing out that when $k_0 = \pi/4,\ 3\pi/8$, and $\pi/2$, such a GWP can approximately propagate along the non-Hermitian SSH chain without spreading [57]. For simplicity, the center momentum k_0 is assumed to be $\pi/4$ in the following, which ensures that the initial state is mainly localized on the upper band of the Hamiltonian H_A with either $\delta > 0$ or $\delta < 0$.

Due to the Eq. (A1) of the Appendix, the initial GWP will travel along the virtual chain a in the absence of the magnetic flux. Actually, at a certain time τ, such a GWP

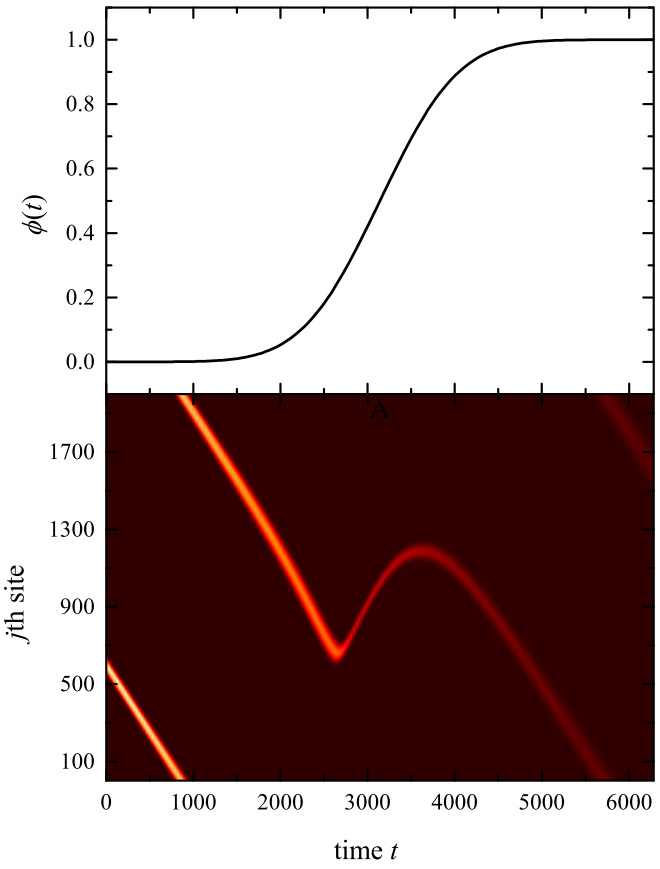

FIG. 5. Numerical simulation of the evolved wave packet driven by the magnetic flux $\phi(t)$ that varies as the error function. The initial state and the system parameters are the same with that of the Fig. 4(c) except that δ is replaced with $-\delta$. Hence the probability of the evolved wave packet is attenuated as time increases.

evolves approximately into

$$\left|G\left(\frac{\pi}{4},\tau\right)\right\rangle \sim \frac{1}{\sqrt{\Omega}}\sum_{l=2N_A+1}^{2N_A+2N_B} e^{-\alpha^2(l-N_c-2v\tau)^2} e^{i\frac{\pi}{4}l}\tilde{c}^{\dagger}_{a,l}|\text{Vac}\rangle \tag{64}$$

in the virtual space, where $v = |(\partial\varepsilon_k/\partial k)_{\pi/2}|$ represents the group velocity of the GWP. From the mapping of the operators (A1)–(A4), we have the final state as

$$\left|G\left(\frac{\pi}{4},\tau\right)\right\rangle = \frac{1}{\sqrt{2}}\sum_{p=1}^{2}\left|G_p\left(\frac{\pi}{4},\tau\right)\right\rangle, \tag{65}$$

where

$$\left|G_p\left(\frac{\pi}{4},\tau\right)\right\rangle = \frac{1}{\sqrt{\Omega}}\sum_{j=1}^{2N_B} e^{-\alpha^2(j-N_\tau)^2} e^{i\frac{\pi}{4}j} c^{\dagger}_{B_p,j}|\text{Vac}\rangle \tag{66}$$

is the clone of the initial GWP with the center $N_\tau \in [1, 2N_B]$. The beam splitter split the single-particle GWP into two cloned GWPs without any reflection. Now we investigate the effect of the magnetic flux threading the ring adiabatically on the dynamics of GWP. We consider the following two cases.

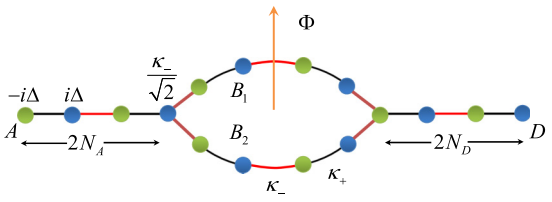

FIG. 6. Schematic illustration of the scattering setup. The scattering system consists of three components: an input non-Hermitian SSH lead A with length N_A, an output non-Hermitian SSH lead D with length N_D, and a ring $\{B_1, B_2\}$ threaded by a magnetic flux $\Phi(t) = 4(N_B + 1/2)\phi(t)$, where N_B represents the length of $B_{1(2)}$. Here $\kappa_+ = -(1-\delta)/2$ and $\kappa_- = -(1+\delta)/2$. The subchains B_1 and B_2 are $\mathcal{P}$ symmetric with respect to the direction of incident GWP. Note that the hopping constants connecting the leads and the scattering ring are modulated with $\kappa_-/\sqrt{2}$, which ensure that the network can be decoupled into two independent virtual chains with different lengths. In the absence of the magnetic flux, therefore, the whole propagation process in the real space is as follows: When the initial GWP reaches the node, it is divided into two identical GWPs which also move with same speed along the legs B_1 and B_2, respectively, without spreading. In the scattering center, the upper and lower GWPs are driven by the effective Hamiltonians which can be constructed by extending the two legs to the completed non-Hermitian SSH rings. The difference between two effective Hamiltonians is the sign of δ resulting from two symmetric legs. This also indicates that when the two GWPs experience half a BO, they acquire the phase difference of π.

B. Perfect transmission

We first consider the case where the magnetic flux ϕ has changed from 0 to π before the GWP enters into the ring. Under this condition, the GWP cannot feel the presence of magnetic flux. Therefore it will travel along the virtual chain a without any reflection. The final state in the virtual space can be expressed as

$$\left|G_p\left(\frac{\pi}{4},\tau_f\right)\right\rangle = \frac{1}{\sqrt{\Omega}}\sum_{l=2N_A+2N_B+1}^{N} e^{-\alpha^2(l-N_f)^2} e^{i\frac{\pi}{4}l}\tilde{c}^{\dagger}_{a,l}|\text{Vac}\rangle, \tag{67}$$

with $N_f \in [2N_A + 2N_B,\ N]$. We detail this process in the Appendix. In the coordinate space, the GWP will pass perfectly through the scattering center. We plot the Fig. 7(a) to demonstrate this case.

C. Partial confinement

Second, we consider the case wheres the magnetic flux ϕ is varied from 0 to π during a wave packet traveling within the ring. In this situation, the initial GWP $|G(\frac{\pi}{4},0)\rangle$ first enters into the ring so that it is split into two cloned GWPs at time τ. When the magnetic flux is switched on, the two cloned GWPs will experience half a BO. However, the corresponding effective driven Hamiltonians are different for two cloned GWPs. For the upper GWP, the effective driven Hamiltonian can be obtained through extending the Hamiltonian H_{B_1} to a complete SSH ring. On the other hand, for a lower GWP, one can check that the effective driven Hamiltonian can be constructed by replacing δ of the upper effective SSH ring with $-\delta$. Therefore, the two cloned GWPs acquire two

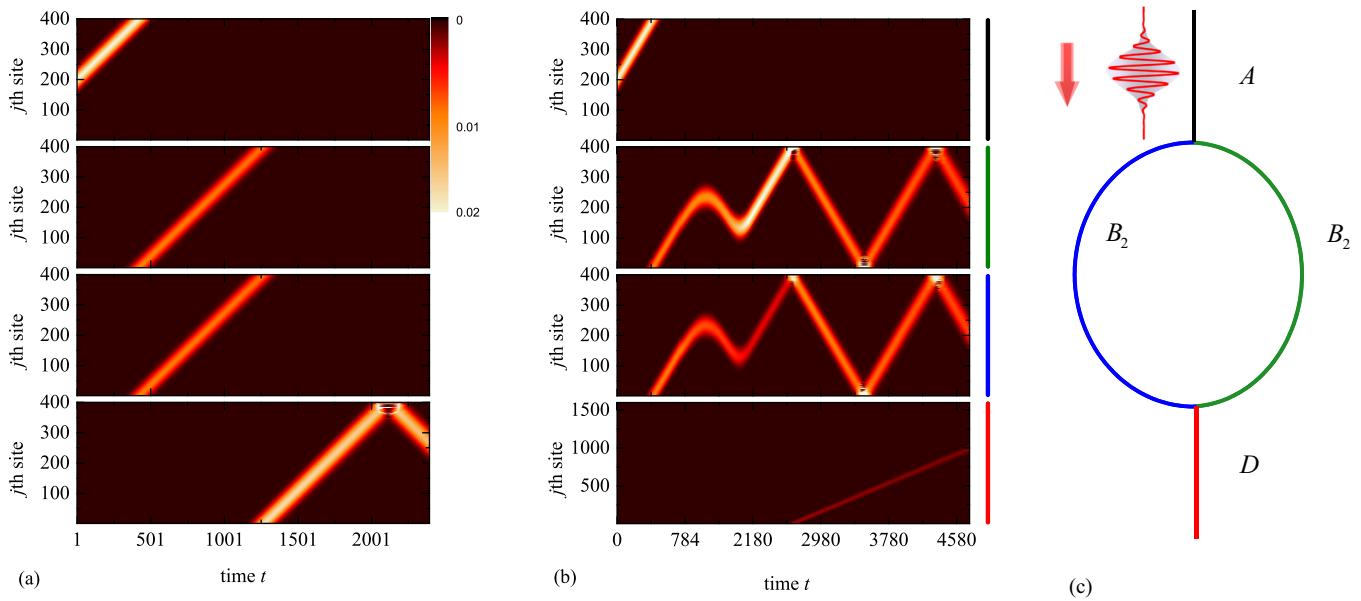

FIG. 7. Propagation of the GWP in the non-Hermitian scattering system with (a) $N_A = N_B = N_D = 400$ and (b) $N_A = N_B = 400$, $N_D = 1600$. The other system parameters are $\Delta = 0.5$ and $\delta = 0.15$. (a) This panel describes the case where the magnetic flux has changed from 0 to π before the GWP enters into the scattering ring. In this condition, the GWP travels along the virtual chain a as shown in the Appendix. Therefore the GWP can pass perfectly through the scattering center with no reflection at the two nodes. In this sense, the non-Hermitian scattering ring is invisible to the incident GWP. (b) When the GWP enters into the scattering ring, the magnetic flux is switched on. In this case, each of the two cloned GWPs undergoes half a BO. The probability of upper GWP is amplified due to $\delta > 0$ of the effective Hamiltonian. On the contrary, the probability of lower GWP is attenuated driven by the corresponding effective Hamiltonian with $\delta < 0$. The adiabatic process bring about a phase difference π between two such cloned GWPs. Therefore, the partial probability of two cloned GWPs is confined in the scattering center, which is inaccordance with our theoretical prediction. (c) Schematic illustration of the concerned scattering system. The four panels of subfigures (a) and (b) represent the input lead A, scattering center $\{B_1, B_2\}$, and output chain D, which are denoted by black, green, blue, and red lines, respectively. Note that the scale of the fourth panel of subfigure (b) is different from the other panels.

opposite adiabatic phase after half a BO. The evolved state can be obtained with the help of Eq. (56) as

$$\left|G\left(\frac{\pi}{4},\tau+\tau_{\mathrm{BO}}\right)\right\rangle = e^{\xi_+}\left|\widetilde{G}_1\left(\frac{\pi}{4},\tau+\tau_{\mathrm{BO}}\right)\right\rangle - e^{-\xi_+}\left|\widetilde{G}_2\left(\frac{\pi}{4},\tau+\tau_{\mathrm{BO}}\right)\right\rangle, \quad (68)$$

where τ_{BO} represents the time that the GWP undergoes half a BO and

$$\left|\widetilde{G}_p\left(\frac{\pi}{4},\tau+\tau_{\mathrm{BO}}\right)\right\rangle = \frac{1}{\sqrt{2\Omega}}\sum_{j=1}^{2N_B}(-1)^j e^{-\alpha^2(j-N_\tau)^2} \times e^{i\frac{\pi}{4}j}c^\dagger_{B_p,j}|\mathrm{Vac}\rangle \quad (69)$$

with the center $N_\tau \in [1, 2N_B]$. Here we ignore the same overall phase $e^{i\alpha^+(\pi)}$ of the two cloned GWPs. From the Eq. (68), we can see that the adiabatic change of the flux leads to a relative π phase between the two cloned GWPs. Straightforward algebra shows that there are $\sinh(\xi_+)$ [$\cosh(\xi_+)$] probability on the virtual chain a (b). This indicates that the partial probability of a wave packet is confined in the scatter which is different from the first case. Note that one can modulate the value of $\Delta\delta$ to reduce the transmission probability and therefore realize the approximate perfect confinement. In Fig. 7(b), we compute the time evolution of the GWP, which is in accordance with our theoretical prediction.

Before closing the discussion of findings, we want to point out the key point to realize the interferometer: The added magnetic flux can make the two identical wave packets experience half a BO so that the two wave packets acquires π phase difference. For a Gaussian wave packet with large half-width (that is, the wave packet is localized in the momentum space), its scattering behavior is only determined by the timing of a flux impulse threading the ring and has nothing to do with the choice of time dependence of the magnetic flux. The type of the time-dependent magnetic flux only influences the trajectory of a wave packet in real space, which can be shown in Figs. 4 and 5. If the magnetic flux varies as $\phi = \mathrm{erf}(t)$, then one needs to increase the size of the scattering center, which ensures the π phase difference between two wave packets. In this sense, the conclusion is independent of the type of time-dependent magnetic flux.

V. SUMMARY

In summary, we have investigated the influence of non-Hermitian term on the Zak phase of Bloch systems. We have shown exactly that for a class of bipartite lattice systems, the real part of the Zak phase cannot be affected by the

staggered imaginary potential. Comparing with the Hermitian system, a nonzero imaginary part appears in the Zak phase. It amplifies and/or attenuates the Dirac norm of the evolved state in the context of dynamical correspondence between the Zak phase and complex Berry phase, in which the Zak phase can be obtained by an adiabatic evolution under the time-dependent threading flux. It is shown that the difference of the real part of a Zak phase is an observable. In this sense, the Zak phase in a non-Hermitian system can still be used to characterize the difference of two topological phases. To further demonstrate this finding, we investigate the scattering problem for a time-dependent scattering center, which is a magnetic-flux-driven non-Hermitian SSH ring. Due to the partial topology of the Zak phase, the intriguing feature of this design are wave-vector independent and allow two distinct dynamical behaviors, perfect transmission or confinement, depending on the timing of a flux impulse threading the ring (scattering center). When the flux is added during a wave packet traveling within the ring, the wave packet is confined in the scatter partially, Otherwise, it exhibits perfect transmission through the scatter. Based on these points, our findings extend the understanding and broaden the possible application of a Zak phase in a non-Hermitian system.

ACKNOWLEDGMENTS

This work was supported by National Natural Science Foundation of China (under Grants No. 11505126 and No. 11874225). X.Z.Z. was also supported by the Ph.D. research startup foundation of Tianjin Normal University under Grant No. 52XB1415 and the Program for Innovative Research in University of Tianjin (under Grant No. TD13-5077).

APPENDIX

The reduction of the scattering system and the corresponding dynamics

To reduce the network of interferometer, the following four sets of fermion operators

$$\tilde{c}^{\dagger}_{a,l} = c^{\dagger}_{A,l}, \tag{A1}$$

$$\tilde{c}^{\dagger}_{a,j+2N_A} = \frac{1}{\sqrt{2}}\left(e^{-i\phi j}c^{\dagger}_{B_1,j} + e^{i\phi j}c^{\dagger}_{B_2,j}\right), \tag{A2}$$

$$\tilde{c}^{\dagger}_{b,j} = \frac{1}{\sqrt{2}}\left(e^{-i\phi j}c^{\dagger}_{B_1,j} - e^{i\phi j}c^{\dagger}_{B_2,j}\right), \tag{A3}$$

$$\tilde{c}^{\dagger}_{d,m} = c^{\dagger}_{D,m}, \tag{A4}$$

for $l \in [1, 2N_A]$, $j \in [1, 2N_B]$, and $m \in [1, 2N_D]$ are introduced to satisfy

$$\left\{\tilde{c}^{\dagger}_{a,j+2N_A},\ \tilde{c}_{b,j}\right\} = 0. \tag{A5}$$

The inverse transformation of the above Eqs. (A1)–(A4) reduces the Hamiltonian (59) into

$$H_{\rm net} = \sum_s \widetilde{H}_s + \widetilde{H}_{\rm joint},$$

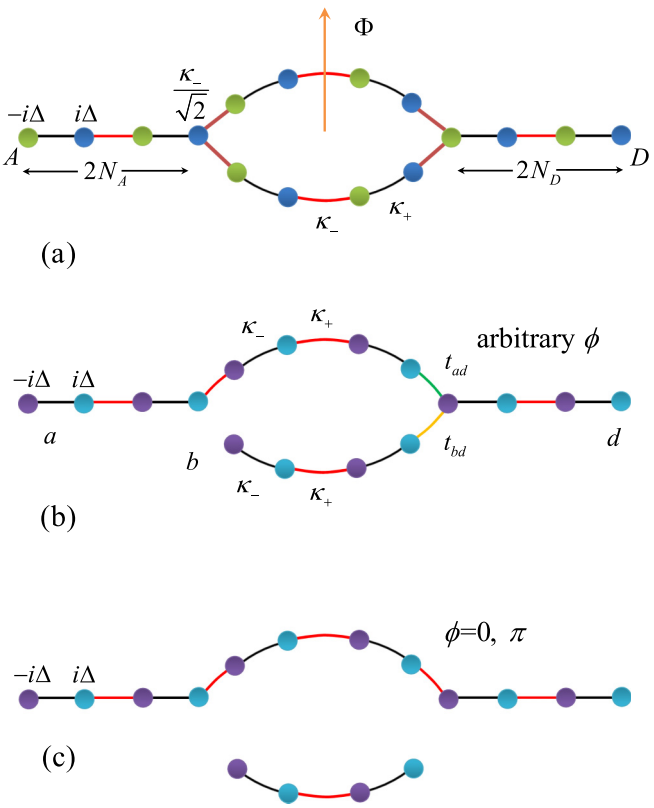

FIG. 8. The ϕ-shaped scattering network with an input non-Hermitian SSH chain A, an output chain non-Hermitian chain D, and a ring $\{B_1, B_2\}$ threaded by a magnetic flux $\Phi(t) = 4(N_B + 1/2)\phi(t)$. (b) For an arbitrary flux, the network can be decoupled into three virtual SSH chains a, b, and d. They connect with each other by the hopping integrals $t_{ad} = (1+\delta)\cos[(2N_b+1)\phi]/2$ and $t_{bd} = -i(1+\delta)\sin[(2N_b+1)\phi]/2$. (c) When $\phi = 0, \pi$, the ϕ-shaped scattering network can be decoupled into a long virtual non-Hermitian SSH chain a with length $N = 2(N_a + N_d)$ and a short virtual non-Hermitian SSH chain b with length $2N_b$.

where

$$\widetilde{H}_s = -\frac{1}{2}\sum_{j=1}^{2N_s-1}[1+(-1)^j\delta](\tilde{c}^{\dagger}_{s,j}\tilde{c}_{s,j+1} + \text{H.c.}) + i\Delta\sum_{j=1}^{2N_s-1}(-1)^j\tilde{c}^{\dagger}_{s,j}\tilde{c}_{s,j}, \tag{A6}$$

$$\widetilde{H}_{\rm joint} = -t_{ad}\tilde{c}^{\dagger}_{a,2N_a}\tilde{c}_{d,1} - t_{bd}\tilde{c}^{\dagger}_{b,2N_b}\tilde{c}_{d,1} + \text{H.c.}, \tag{A7}$$

with $s = a$, b, and d. The couplings are $t_{ad} = (1+\delta)\cos[(2N_B+1)\phi]/2$ and $t_{bd} = iJ(1+\delta)\sin[(2N_B+1)\phi]/2$, respectively. For clarity, we sketch this decomposition in Fig. 8. It is shown that for an arbitrary flux ϕ, the concerned network can be decoupled into three virtual non-Hermitian SSH chains a, b, and d with length $N_a = N_A + N_B$, $N_b = N_B$, and $N_d = N_d$, respectively. The virtual chains a and b connect with chain d through the hopping integral t_{ad} and t_{bd}, which depends on the magnetic flux ϕ. In the following, we focus on the case that $\phi = 0$ or π. Under this condition, the virtual chains b and d are decoupled. The network reduced to two independent non-Hermitian SSH

chains with lengths $N = 2N_a + 2N_d$ and $2N_b$, respectively. Then the corresponding Hamiltonian can be given as

$$\begin{aligned} H_{\text{net}} = & -\frac{1}{2}\sum_{j=1}^{2N-1}[1+(-1)^j\delta](\tilde{c}^{\dagger}_{a,j}\tilde{c}_{a,j+1}+\text{H.c.}) \\ & +i\Delta\sum_{j=1}^{2N-1}(-1)^j\tilde{c}^{\dagger}_{a,j}\tilde{c}_{a,j}, \\ & -\frac{1}{2}\sum_{j=1}^{2N_b-1}[1+(-1)^j\delta](\tilde{c}^{\dagger}_{b,j}\tilde{c}_{b,j+1}+\text{H.c.}) \\ & +i\Delta\sum_{j=1}^{2N_b-1}(-1)^j\tilde{c}^{\dagger}_{b,j}\tilde{c}_{b,j}, \end{aligned} \tag{A8}$$

with the defined operators

$$\tilde{c}^{\dagger}_{a,2N_A+2N_B+m} = \tilde{c}^{\dagger}_{d,m}. \tag{A9}$$

This fact means that for an arbitrary initial state localized on the virtual chain $a(b)$, it will evolve driven by the virtual chain of length $N(2N_b)$. There are two typical features that should be mentioned: (i) For the state localized on the virtual chain a, the evolve state will exhibit perfect transmission through the scattering center. (ii) For the state localized on the virtual chain b, the localized state will be confined in the scattering center. These two mechanisms are crucial to understand the wave-packet dynamics.

[1] C. M. Bender and S. Boettcher, Phys. Rev. Lett. **80**, 5243 (1998).
[2] C. M. Bender, D. C. Brody, H. F. Jones, and B. K. Meister, Phys. Rev. Lett. **98**, 040403 (2007).
[3] C. M. Bender, Rep. Prog. Phys. **70**, 947 (2007).
[4] R. El-Ganainy, K. G. Makris, D. N. Christodoulides, and Z. H. Musslimani, Opt. Lett. **32**, 2632 (2007).
[5] K. G. Makris, R. El-Ganainy, D. N. Christodoulides, and Z. H. Musslimani, Phys. Rev. Lett. **100**, 103904 (2008).
[6] Z. H. Musslimani, K. G. Makris, R. El-Ganainy, and D. N. Christodoulides, Phys. Rev. Lett. **100**, 030402 (2008).
[7] A. Guo, G. J. Salamo, D. Duchesne, R. Morandotti, M. Volatier-Ravat, V. Aimez, G. A. Siviloglou, and D. N. Christodoulides, Phys. Rev. Lett. **103**, 093902 (2009).
[8] C. E. Rüter, Nat. Phys. **6**, 192 (2010).
[9] A. Ruschhaupt, F. Delgado, and J. G. Muga, J. Phys. Math. Gen. **38**, L171 (2005).
[10] S. Klaiman, U. Günther, and N. Moiseyev, Phys. Rev. Lett. **101**, 080402 (2008).
[11] T. Kottos, Nat. Phys. **6**, 166 (2010).
[12] S. Longhi, Laser Photon. Rev. **3**, 243 (2009).
[13] A. Mostafazadeh, Phys. Rev. Lett. **102**, 220402 (2009).
[14] A. Mostafazadeh, Phys. Rev. A **80**, 032711 (2009).
[15] M. S. Rudner and L. S. Levitov, Phys. Rev. Lett. **102**, 065703 (2009).
[16] K. Esaki, M. Sato, K. Hasebe, and M. Kohmoto, Phys. Rev. B **84**, 205128 (2011).
[17] S. Malzard, C. Poli, and H. Schomerus, Phys. Rev. Lett. **115**, 200402 (2015).
[18] C. Yuce, Phys. Lett. A **379**, 1213 (2015).
[19] C. Yuce, Eur. Phys. J. D **69**, 184 (2015).
[20] A. K. Harter, T. E. Lee, and Y. N. Joglekar, Phys. Rev. A **93**, 062101 (2016).
[21] T. E. Lee, Phys. Rev. Lett. **116**, 133903 (2016).
[22] S. Weimann, M. Kremer, Y. Plotnik, Y. Lumer, S. Nolte, K. G. Makris, M. Segev, M. C. Rechtsman, and A. Szameit, Nat. Mater. **16**, 433 (2017).
[23] S. Y. Yao and Z. Wang, Phys. Rev. Lett. **121**, 086803 (2018).
[24] C. Yin, H. Jiang, L. Li, R. Lü, and S. Chen, Phys. Rev. A **97**, 052115 (2018).
[25] S. Lieu, Phys. Rev. B **97**, 045106 (2018).
[26] C. Li, X. Z. Zhang, G. Zhang, and Z. Song, Phys. Rev. B **97**, 115436 (2018).
[27] V. M. Martinez Alvarez, J. E. Barrios Vargas, and L. E. F. Foa Torres, Phys. Rev. B **97**, 121401(R) (2018).
[28] H. Shen, B. Zhen, and L. Fu, Phys. Rev. Lett. **120**, 146402 (2018).
[29] F. K. Kunst, E. Edvardsson, J. C. Budich, and E. J. Bergholtz, Phys. Rev. Lett. **121**, 026808 (2018).
[30] Y. Xiong, J. Phys. Commun. **2**, 035043 (2018).
[31] R. Wang, X. Z. Zhang, and Z. Song, Phys. Rev. A **98**, 042120 (2018).
[32] B. Zhu, R. Lü, and S. Chen, Phys. Rev. A **89**, 062102 (2014).
[33] S. Yao, F. Song, and Z. Wang, Phys. Rev. Lett. **121**, 136802 (2018).
[34] Z. Turker, S. Tombuloglu, and C. Yuce, Phys. Lett. A **382**, 2013 (2018).
[35] L. Zhou, Q. H. Wang, H. Wang, and J. Gong, Phys. Rev. A **98**, 022129 (2018).
[36] H. Menke and M. M. Hirschmann, Phys. Rev. B **95**, 174506 (2017).
[37] B. X. Wang and C. Y. Zhao, Phys. Rev. A **98**, 023808 (2018).
[38] F. Dangel, M. Wagner, H. Cartarius, J. Main, and G. Wunner, Phys. Rev. A **98**, 013628 (2018).
[39] R. Okugawa and T. Yokoyama, arXiv:1810.03376.
[40] D. Leykam, K. Y. Bliokh, C. Huang, Y. D. Chong, and F. Nori, Phys. Rev. Lett. **118**, 040401 (2017).
[41] J. Zak, Phys. Rev. Lett. **62**, 2747 (1989).
[42] J. C. Garrison and E. M. Wright, Phys. Lett. A **128**, 177 (1988).
[43] G. Dattoli, R. Mignani, and A. Torre, J. Phys. A **23**, 5795 (1990).
[44] C. Z. Ning and H. Haken, Phys. Rev. Lett. **68**, 2109 (1992).
[45] D. J. Moore and G. E. Stedman, Phys. Rev. A **45**, 513 (1992).
[46] M. Pont, R. M. Potvliege, R. Shakeshaft, and P. H. G. Smith, Phys. Rev. A **46**, 555 (1992).
[47] S. Massar, Phys. Rev. A **54**, 4770 (1996).
[48] Y. C. Ge and M. S. Child, Phys. Rev. A **58**, 872 (1998).
[49] R. S. Whitney, Y. Makhlin, A. Shnirman, and Y. Gefen, Phys. Rev. Lett. **94**, 070407 (2005).

[50] H. Mehri-Dehnavi and A. Mostafazadeh, J. Math. Phys. **49**, 082105 (2008).
[51] J. K. Chin, D. E. Miller, Y. Liu, C. Stan, W. Setiawan, C. Sanner, K. Xu, and W. Ketterle, Nature (London) **443**, 961 (2006).
[52] N. Strohmaier, Y. Takasu, K. Günter, R. Jördens, M. Köhl, H. Moritz, and T. Esslinger, Phys. Rev. Lett. **99**, 220601 (2007).
[53] L. Hacke, Science **327**, 1621 (2010).
[54] S. Longhi, Phys. Rev. A **88**, 052102 (2013).
[55] W. H. Hu, L. Jin, and Z. Song, Quantum Inf. Process **12**, 3569 (2013).
[56] S. Lin, X. Z. Zhang, and Z. Song, Phys. Rev. A **90**, 063411 (2014).
[57] W. H. Hu, L. Jin, Y. Li, and Z. Song, Phys. Rev. A **86**, 042110 (2012).